RADIO FREQUENCY RESONANCES INSIDE A HUMAN HEAD

Denys Nikolayev

Department of Theory of Electrical Engineering, University of West Bohemia, Czech Republic;
ITRE, Lviv Polytechnic National University, Ukraine
d@deniq.com

Abstract: RF equipment compliance tests employ electromagnetic field calculation in a head phantom to derive Specific Absorption Rate values. We have hypothesized that a biological tissue in certain conditions could act like a dielectric resonator hence affecting the field estimation. To study the resonance effects in a human head, we have formulated an eigenfrequency problem for a structurally realistic 2D human head phantom and solved it by the finite element method. The results have revealed 124 underdamped eigenfrequencies within a 0,2–2 GHz frequency band.

Key words: eigenfrequency, brain, phantom, mobile phone, finite element method.

1. Introduction

Rapid development of mobile telecommunication systems caused a lot of debates around its impact on health. While we have modest historical experience about biological reaction on lasting RF exposure, thermal effects of non-ionizing radiation proved to be harmful long ago and arguments still center around non-thermal effects [1-4]. Thousands of studies have been carried out aimed at investigating RF exposure effects, many of them are still ongoing [5]. Based on the results, several institutions established guidelines to limit public exposure; IEEE [6] and ICNIRP [7] are those mostly used.

Almost all modern standards adopted the index of Specific Absorption Rate (SAR) as a quantitative measure of the energy absorbed in a biological tissue:

$$\text{SAR} = \int (\sigma(\mathbf{r})|\mathbf{E}(\mathbf{r})|^2/\rho(\mathbf{r}))d\mathbf{r}, \qquad (1)$$

where σ is the tissue electrical conductivity [S/m], $\mathbf{E}$ denotes the root mean square electric field [V/m], ρ stands for the tissue density [Kg/m³], and $\mathbf{r}$ is the general space variable.

Ukraine and Russia, however, employ Poynting vector to standardize the exposure limits defined as

$$\overline{S} = |\mathbf{E}|^2/\eta = \eta|\mathbf{H}|^2, \qquad (2)$$

where η is the wave impedance ($\cong 337\Omega$ for free space).

Procedures IEEE 1528-2013 [8] and IEC 62209-1 [9] describe how to measure peak spatial-average SAR of hand-held devices used in close proximity to the ear. However, neither of the described approaches considers possible resonance effects inside a human head due to substantial difference in dielectric properties of its tissues (see table 1). Moreover, the proposed head phantoms make impossible to study these effects due to homogenization and averaging of its structure.

Based on the theory of dielectric resonators [10], we asked whether underdamped resonances do exist in a head within VHF–SHF frequency bands. It may be possible due to electrically heterogeneous brain structure with differences of ε_r up to 63,13 on the CSF/marrow boundary, which could be seen in Table 1.

Dielectric resonators are similar in principle to the cavity resonators but have field fringing on the sides and ends that lowers quality factor Q_{fact} [11]. The example in Fig. 1 demonstrates a cylindrical dielectric resonator.
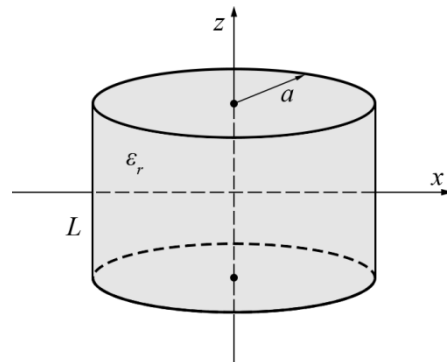

Fig. 1. Geometry of a cylindrical dielectric resonator.
L: height, a: radius, and ε_r: relative permittivity.

Estimated resonant frequencies of TM_{mnp} modes could be obtained from the following equation for a dielectric cylindrical resonator (a, L) [10]:

$$f_r\left(\text{TM}_{mnp}\right) = \frac{1}{2\pi\sqrt{\mu\varepsilon}}\left[\left(\frac{x_{mn}}{a}\right)^2 + \left(\frac{p\pi}{L}\right)^2\right]^{1/2} \quad (3)$$

where x_{mn} denotes the zeros of the mth order Bessel function while n is its number of zero crossings, μ is the absolute permeability, and ε_r is the absolute permittivity. Thus, from (3) for an adult with the head radius of $a \cong 9$ [cm], the first resonant frequency f_{TM010} [Hz] is located roughly at

$$\frac{1}{2\pi\sqrt{1,25\times10^{-6}\cdot40\cdot8,9\times10^{-12}}}\frac{2,4048}{0,09} \approx 2\times10^8. \quad (4)$$

In this way, 200 MHz defines the lower bound for the eigenfrequency study of a human head. The upper bound may be estimated from the skin penetration depth that could be found in [12, 13]. At 2 GHz, the penetration depth for skin is 0,026 m, so it is beside the purpose to search for eigenfrequencies further.

Eigenfrequency study of a realistic human head phantom for the defined frequency band of 0,2–2 GHz could be realized only by using numerical methods due to the complex geometry of the problem. The finite element method is more appropriate for this kind of problem than Finite-Difference Time-Domain (FDTD) method because of its adaptivity [14] and better boundary approximation. In both cases, the study domain requires truncating using either appropriate boundary conditions or perfectly matched layers.

As this study aims to found the existence of underdamped resonances in a human head caused by sinuous brain structure, it is sufficient to formulate the problem in 2D assuming $\mathbf{E}(z) = $ const., i.e. find only the frequencies for TM_{mn0} modes. As it could be easily seen from (3), for the 3D case when $a \approx L$, there will be approximately 33% more eigenfrequencies within the defined frequency band.

2. Phantom geometry modeling

We used a simulated normal brain MRI scan [15] (Fig. 2: left) to create a 2D realistic brain phantom model for electromagnetic eigenfrequency analysis. The advantage of the simulated MRI scans is that the different tissues could be easily separated to layers and converted to lines using image processing algorithms. After tracing each image layer using MATLAB, we obtained the paths of all boundaries between tissues within a head and combined them to the final geometrical model (Fig. 2: right). Then, the geometry is ready to be exported to FEM software for assigning material properties, boundary conditions and, finally, for computation.
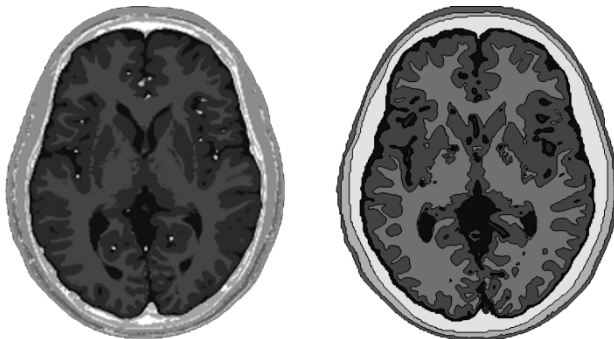

Fig. 2. MRI head scan simulation [15] (left)
and resulted model (right).

A detailed process of a 2D and 3D head phantom development algorithm for FEM study is out of the scope of this paper and will be published separately.

3. Mathematical model

To find eigenvalues in a frequency domain using COMSOL implementation of the finite element method [16], the governing wave function for the problem could be written as

$$\nabla \times \frac{1}{\mu_r}\left(\nabla \times \mathbf{E}\right) - k_0^2\left(\varepsilon_r - \frac{j\sigma}{\omega\varepsilon_0}\right)\mathbf{E} = 0 , \quad (5)$$

where μ_r and ε_r are respectively relatives permeability and permittivity, σ is the electrical conductivity [S/m], ε_0 stands for the electric constant [F/m], ω denotes the frequency [rad/s], and k_0 is the wave number of free space that is defined as

$$k_0 = \omega\sqrt{\varepsilon_0\mu_0} = \omega/c . \quad (6)$$

Boundary conditions between two media (σ_i, ε_i, μ_i, where $i = 1, 2$) are defined as

$$\begin{aligned}
\hat{\mathbf{n}} \times \left(\mathbf{E}_1 - \mathbf{E}_2\right) &= 0 \\
\hat{\mathbf{n}} \times \left(\mathbf{H}_1 - \mathbf{H}_2\right) &= \mathbf{J}_s \\
\hat{\mathbf{n}} \cdot \left(\mathbf{D}_1 - \mathbf{D}_2\right) &= \rho_s \\
\hat{\mathbf{n}} \cdot \left(\mathbf{B}_2 - \mathbf{B}_1\right) &= 0
\end{aligned} , \quad (7)$$

where $\mathbf{J}_s$ is the current density at the boundary [A/m] and ρ_s denotes the surface charge density [C/m²].

As we deal with lossy medium (i.e. the conduction current is not negligible), the eigenvalue λ is complex and consists of eigenfrequency and damping in space/time. The quality factor could be derived from eigenfrequency ω [rad/s] and damping δ as

$$Q_{\text{fact}} = \frac{\omega}{2|\delta|} . \quad (8)$$

Physical meaning of Q_{fact} is the ratio of the stored energy to the energy dissipated over one radian of oscillation.

4. Head tissue properties

Biological tissues are dispersive since the electrical properties vary with frequency f [17]. A linear dependence has been assumed for the studied bandwidth. Table 1 shows the linear approximations for the properties of the tissues used in the model.

Table 1

Linear approximation for the head tissue electric properties

Tissue	Rel. permittivity ε_r [–]	Electrical conductivity σ [S/m]
Blood	$-2\times10^{-9}f + 63{,}348$	$6\times10^{-10}f + 1{,}0323$
White Matter	$-2\times10^{-9}f + 40{,}761$	$4\times10^{-10}f + 0{,}2666$
Grey Matter	$-3\times10^{-9}f + 55{,}371$	$5\times10^{-10}f + 0{,}4932$
Cerebrospinal Fluid	$-2\times10^{-9}f + 70{,}076$	$6\times10^{-10}f + 1{,}9016$
Marrow	$-1\times10^{-10}f + 5{,}637$	$3\times10^{-11}f + 0{,}0119$
Skull	$-2\times10^{-9}f + 22{,}233$	$3\times10^{-10}f + 0{,}0917$
Skin (*incl.* Muscles)	$-2\times10^{-9}f + 48{,}31$	$4\times10^{-10}f + 0{,}4573$

f denotes the frequency [Hz].

5. FEM Computation

The problem was solved in 2D formulation for the out-of-plane electric field component (E_z) using COMSOL 4.3b. The discretization gives 115 846 elements using automatic space adaptivity, including 115 702 triangular and 144 quadrilateral (Fig. 3). Linear shape functions were used for the solution $\phi(x,y)$ interpolation inside the element. In this way, the number of degrees of freedom (DoF) of the model will be reduced without significant loss in accuracy due to very fine mesh ($L_{elem} \ll \lambda$ [m]) that is imposed by the geometry of the problem. For a triangular element, the solution interpolation is given by

$$\phi(x,y) = N_i(x,y)\phi_i + N_j(x,y)\phi_j + N_k(x,y)\phi_k \quad (9)$$

where $N_{i,j,k}$ are Lagrange polynomial coefficients [18] and $\phi_{i,j,k}$ denote the values at the nodes.
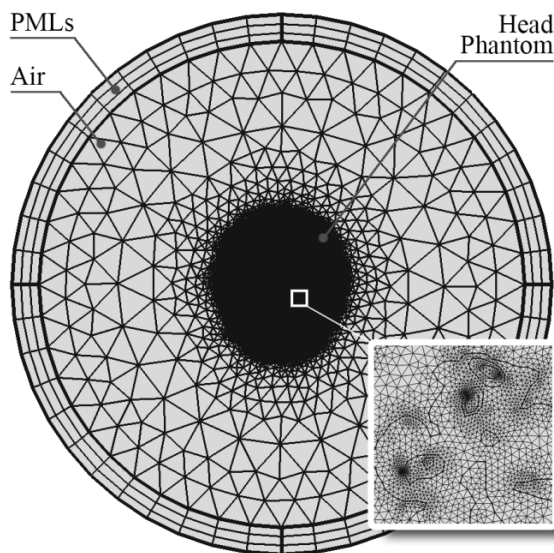

Fig. 3. Adaptive finite element discretization of the problem using triangular and quadrilateral elements.

The study area was truncated using a perfectly matched layer (PML) that absorbs all radiated waves with negligible reflections by stretching virtual domains into a complex plane. It is done by using coordinate transform for the general space variable r:

$$r' = (r/\Delta_w)^n (1-j)F, \quad (10)$$

where Δ_w is the width of PML region, *n* represents the PML order and F denotes the scaling factor.
In order to linearize the eigenvalue problem, perfect electric conductor boundary condition ($\hat{\mathbf{n}} \times \mathbf{E} = 0$) was imposed at the outer limits of PML.

PMLs should be sufficiently away from the phantom to compute the correct eigenvalues, but putting it too far will affect the number of DoFs and thus the computation performance. The variation of eigenvalues decays exponentially with PML radius, so the rule of thumb

is to select such a radius that will be sufficiently accurate; for our case we chose 0,4 m.

The resulting model has 58 020 degrees of freedom; the solution time is about 20 seconds when searching for five eigenfrequencies on Intel i5 2520M processor with 16 Gb of RAM.

6. Method validation

If we consider an *L*-infinite cylinder of radius *a*, the second term in the brackets in (3) disappears hence the resonator would support only TM$_{mn0}$ modes and the problem dimension could be reduced to 2D. In this way, we can verify the method adequacy by comparing the analytical approximation with numerical approach. So, we have considered the dielectric resonator ($\varepsilon_r = 70$) with the radius $a = 0,05$ m. The analytical approximation is:

$$f_{TM_{010}} \approx 1/2\pi\sqrt{1,25 \times 10^{-6} \cdot 70 \cdot 8,85 \times 10^{-12} \times}$$
$$\times 2,4048/0,05 \approx 2,74 \times 10^8 \,[\text{Hz}] \quad (11)$$

The actual resonant frequency — and so its numerical estimation — would be slightly lower because of the field fringing on the resonator sides.

The numerical solution (Fig. 4) gives

$$f_{TM_{010}} \approx 2,697 \times 10^8 \,[\text{Hz}]$$

which proves the adequacy of the modeling approach and its sufficient accuracy for the given problem.
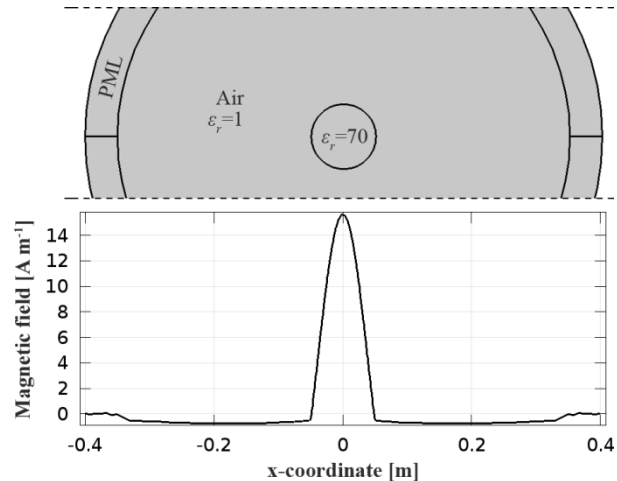

Fig. 4. FEM computation of TM$_{010}$ mode for the cylindrical dielectric resonator with the radius a=0,05 m.

However, FEM eigenfrequency solver would also find some resonances occurring in-between PML and resonator, which are incorrect for the physical object. These could be easily filtered during post-processing by comparing electromagnetic fields inside and outside the resonator. Moreover, the problems with complicated geometry and many DoFs may generate some erroneous results. To filter them out, it is necessary to visually check the field distributions of the eigenfrequencies found.

7. Results

The analysis over the frequency band 0,2–2 GHz found 124 proper eigenfrequencies, i.e. the eigenfrequencies that are invariant to the size of PML. The observable erroneous results due to numerical approximation were also filtered. All eigenfrequencies are the TM_{mn0} type modes due to 2D formulation of the problem.

A statistical analysis of the results in Fig. 5 shows nonperiodic eigenfrequencies frequency distribution. It is hardly possible to predict where the next eigenfrequency in the spectrum would occur, which is caused by complex geometry of the problem.
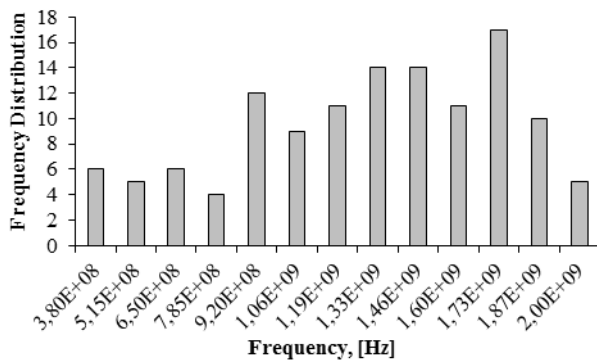

Fig. 5. Frequency distribution of eigenfrequencies in the realistic 2D model of human head phantom.

We can notice the peaks of eigenfrequencies in comparison with neighbors for the bins 920 MHz and 1,73 GHz. This could be interpreted as higher probability of resonance at the frequency range of these bins.
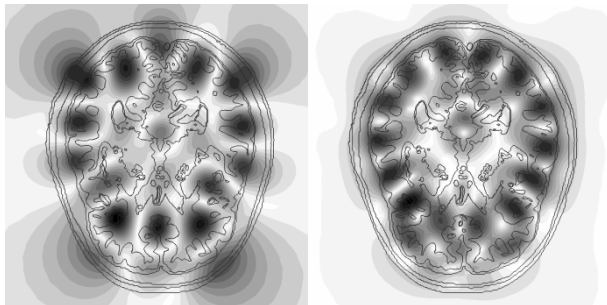

*Fig. 6. Example of numerical computation of eigenfrequencies in the human head phantom at 905 MHz; left: electric field **E**, right: magnetic field **H**. $Q_{fact} = 2,6$.*

Fig. 6 and Fig. 7 show examples of electric and magnetic field distributions for the eigenfrequencies 905 MHz and 1,775 GHz. These frequencies belong to GSM900 and DSC1800 uplink bandwidths respectively and thus a mobile phone operating close to the head phantom could potentially rouse a resonance given proper coupling conditions and rather high quality factor. Q_{fact} for the studied model is approx. 2,7±0,9, which means we deal with an underdamped system ($Q_{fact} > \frac{1}{2}$) for all the eigenfrequencies found in the study.
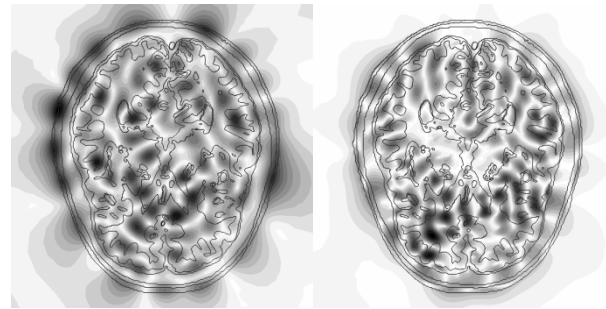

*Fig. 7. Example of numerical computation of eigenfrequencies in the human head phantom at 1,775 GHz; left: electric field **E**, right: magnetic field **H**. $Q_{fact} = 3,4$.*

8. Discussion and Conclusion

This study has found that resonances specific for sinuous brain structure do exist in a realistic human head phantom. The statistical analysis of the data showed that the frequency distribution of eigenfrequencies is random with some peaks: around 920 MHz and 1,73 GHz for this study. The exact distribution of the peaks depends on individual morphology of the head/ brain and will vary according to different subjects. Thereby, there might be subjects that have the peaks around operating frequencies of mobile telephony standards. If a phone is held near a head it could excite the resonances; this might explain cases of individual electromagnetic sensibility. In this case, a patient must be sensible not only to the distance to a source, but also to its position around the head and the fluctuations of frequency.

While eigenfrequency analysis proves the existence of resonance frequencies in the head that could not be found using current procedures, it has some limitations. The major one is the inability to analyze couplings with source(s) and thus predict whether the resonance could be excited. Among other limitations, even if the resonance could be excited by an external source, it is impossible to assess how much the level of exposure will rise. These define the future study directions. It should be also noted, that solving the same problem in 3D will extend the density of eigenfrequencies in the studied frequency band. This also needs confirming despite the fact that it could be a very long computation.

The findings of the study of electromagnetic eigenfrequencies in the head could be used not only for modifying SAR measurement procedures, but also for the development of new medical imaging and monitoring techniques that measure changes in the body using the fluctuations of eigenfrequency spectrum.

Our heads may be resonant with the frequencies used nowadays in mobile telecommunications; as a result, SAR measurements might vary for the same device depending on its frequency and exact position. We highly anticipate that it will be considered in the next revisions of the exposure determination procedures.

References

[1] R. Baan, Y. Grosse, B. Lauby-Secretan, F. El Ghissassi, V. Bouvard, L. Benbrahim-Tallaa*, et al.*, "Carcinogenicity of radiofrequency electromagnetic fields", *The Lancet Oncology,* vol. 12, pp. 624–626, 2011.

[2] D. Poljak, *Human exposure to electromagnetic fields*. UK: WIT Press, 2004.

[3] M. H. Repacholi, A. Lerchl, M. Röösli, Z. Sienkiewicz, A. Auvinen, J. Breckenkamp*, et al.*, "Systematic review of wireless phone use and brain cancer and other head tumors", *Bioelectromagnetics,* pp. 187–206, 2011.

[4] The International Comission on Non-Ionizing Radiation Protection, "General approach to protection against non-ionizing radiation", *Health Physics,* vol. 82, pp. 540–548, 2002.

[5] World Health Organization. (2013). *Electromagnetic Field Research Database.* Available: http://www.who.int/peh-emf/research/database/en/

[6] IEEE, "IEEE Standard for Safety Levels with Respect to Human Exposure to Radio Frequency Electromagnetic Fields, 3 kHz to 300 GHz", vol. C95.1-2005, ed. New York, NY: IEEE, 2005.

[7] The International Commission on Non-Ionizing Radiation Protection, "Guidelines for limiting exposure to time-varying electric, magnetic, and electromagnetic fields (up to 300 GHz)", *Health Physics,* vol. 74, pp. 494–522, 1998.

[8] IEEE, "IEEE Recommended Practice for Determining the Peak Spatial-Average Specific Absorption Rate (SAR) in the Human Head from Wireless Communications Devices: Measurement Techniques", in *IEEE Std 1528-2013 (Revision of IEEE Std 1528-2003)* vol. IEEE Std 1528-2013 (Revision of IEEE Std 1528-2003), ed, 2013, p. 246.

[9] IEC, "Human exposure to RF fields from hand-held and body-mounted wireless communication devices—Human models, instrumentation, and procedures—Part 1: Procedure to determine the SAR for hand-held devices used in close proximity to the ear (frequency range of 300 MHz to 3 GHz)", vol. IEC 62209-1 ed 1.0, ed, 2005.

[10] D. Kajfez and P. Guillon, *Dielectric resonators*. Dedham, MA: Artech House, 1986.

[11] D. M. Pozar, *Microwave engineering*, 4th ed. Hoboken, NJ, USA: Wiley, 2012.

[12] S. Gabriel, R. W. Lau, and C. Gabriel, "The dielectric properties of biological tissues: II. Measurements in the frequency range 10 Hz to 20 GHz", *Phys Med Biol,* vol. 41, pp. 2251–2269, Nov 1996.

[13] S. Gabriel, R. W. Lau, and C. Gabriel, "The dielectric properties of biological tissues: III. Parametric models for the dielectric spectrum of tissues", *Phys Med Biol,* vol. 41, pp. 2271–2293, Nov 1996.

[14] P. Solin, K. Segeth, and I. Dolezel, *Higher-Order Finite Element Methods*. London, UK: Chapman and Hall/CRC, 2003.

[15] B. Aubert-Broche, A. C. Evans, and L. Collins, "A new improved version of the realistic digital brain phantom", *NeuroImage,* vol. 32, pp. 138–145, 8/1/2006.

[16] J.-M. Jin, *The finite element method in electromagnetics*, 2nd ed. New York, USA: John Wiley & Sons, 2002.

[17] C. Gabriel, "Compilation of the Dielectric Properties of Body Tissues at RF and Microwave Frequencies", King's College London, Physics Department AUOE-TR-1996-0037, June 1996.

[18] R. L. Burden and J. D. Faires, *Numerical analysis*, 9th ed. Boston, MA, USA: Brooks/Cole, Cengage Learning, 2011.

РАДІОЧАСТОТНІ РЕЗОНАНСИ У ГОЛОВІ ЛЮДИНИ

Денис Ніколаєв

Для сертифікації побутових радіопристроїв на відповідність гранично допустимим нормам випромінювання використовують розрахунок поля у фантомі голови людини для визначення питомого коефіцієнту поглинання електромагнітної енергії. Ми припустили, що особливості побудови тканин голови можуть підтримувати специфічні резонанси і, таким чином, впливати на розподіл поля та, відповідно, на питомий коефіцієнт поглинання електромагнітної енергії. Для вивчення резонансних явищ у голові людини ми сформулювали задачу розрахунку власних частот для структурно-реалістичного двовимірного фантому та розв'язали її методом скінчених елементів. Аналіз виявив 124 власні частоти з високою добротністю у діапазоні частот 0,2–2 ГГц.

Denys Nikolayev is a postgraduate student at the Department of Theory of Electrical Engineering at the University of West Bohemia (Czech Republic) and a C.Sc. candidate at Lviv Polytechnic National University (Ukraine). His research interests include computational electromagnetics, higher order numerical and hybrid methods for RF engineering, coupled problems, and its biomedical applications.